Calculated And Measured Air-Kerma Response Of Ionization Chambers In Low- And Medium-Energy Photon Beams

J. P. Seuntjens,[1] I. Kawrakow,[2] J. Borg,[3] F. Hobeila,[1] and D. W. O. Rogers[2]
[1] *Medical Physics Unit, McGill University, Montreal, Quebec, Canada*
[2] *Ionizing Radiation Standards, National Research Council, Ottawa, Ontario, Canada*
[3] *Radiation Physics, Princess Margaret Hospital, Toronto, Ontario, Canada*

Introduction

For reasons of precision and stability, gas-filled ionization chambers are currently still used as the main instruments to perform clinical reference dosimetry, and very often are used to perform relative dosimetry measurements. For the calculation of the response of ion chambers in high-energy photon beams use is made of the Spencer-Attix cavity theory. This theory works rather well for chamber response calculations in high-energy photon beams under conditions of electron equilibrium. However, there are many types of situations under which the theory does not work properly and Monte Carlo methods, provided accurate, are an important alternative.

When a chamber is embedded in a medium, its response R in terms of absorbed dose can be defined as the ratio of absorbed dose to the medium at the effective point of measurement to the average absorbed dose in its cavity gas D_{gas}, i.e.,

$$R = \frac{D_{gas}}{D_m} = f_{c,m}. \tag{1}$$

In this context, in cavity theories, R is often noted as $f_{c,m}$. When a chamber is used to measure air-kerma K_{air}, its response is similarly expressed as

$$R = \frac{D_{gas}}{K_{air}}. \tag{2}$$

D_{gas} is proportional to the signal measured in the chamber. The effective volume of the gas in the chamber is involved in the proportionality factor. Note that for air-filled chambers, the energy dependence of the average energy required to produce an ion pair in air, W/e, is usually ignored.

Calculation of ion chamber response using condensed history Monte Carlo techniques is traditionally considered to be one of the most stringent tests of the way the code handles the electron transport (Nahum 1989). Inaccuracies in the handling of the electron transport usually show up as dependencies of the result on the electron step size. In EGS4 terminology, one would traditionally perform a study of the results for different values of ESTEPE (the maximum fractional energy loss per step allowed) or impose an SMAX (a maximum step length allowed). With the goal to perform reliable calculations of ion chamber response, the PRESTA algorithm was developed (Bielajew and Rogers 1986, 1987) to resolve the so-called step-size artifact. For a large class of problems, this algorithm indeed relaxed restrictions on step size that otherwise would provoke calculation errors or a prohibitively intensive CPU time consumption. For a while after PRESTA's development with the limited CPU power available, it seemed that within estimated uncertainties, chamber response could be calculated accurately under appropriate ESTEPE restrictions.

However in 1993, Rogers (1993) showed that systematic problems of the order of 1% were still present in chamber response calculations for low-Z cavities at ^{60}Co and chamber response was found to be strongly step-size dependent for 200 keV photon radiation. The study was performed by comparing Monte Carlo calculated chamber response with Spencer-Attix cavity theory predictions and showed that the Monte Carlo calculations overpredicted the response by 1% for ^{60}Co photons. Contrary to the ^{60}Co results, where it was believed that the Spencer-Attix theory was accurate to better than a few tenths of a percent, an arbitrarily normalized calculation of chamber response at 200 keV was shown, since cavity theory was not expected to be valid at these low energies.

To address these and other known problems with the EGS4/PRESTA system, Kawrakow (Kawrakow and Bielajew 1998a,b; Kawrakow 2000a,b) developed a new electron transport algorithm and incorporated it, together with other important improvements in photon physics, into the new version of EGS, EGSnrc (Kawrakow and Rogers 2000). The electron transport algorithm has following features: (i) it is based on a new any-angle multiple scattering theory (Kawrakow and Bielajew 1998a); (ii) it incorporates an improved electron-step algorithm; (iii) the fictitious method for sampling distances between discrete interactions was corrected; (iv) the evaluation of energy loss has been made more accurate; (v) an exact ("analog") boundary crossing algorithm was implemented. In an associated paper, Kawrakow (2000b) proved that, for the ion chamber response problem, EGSnrc produces results consistent at the 0.1% level for Al and C walled chambers at ^{60}Co energies. The differential effect of various improvements in the electron transport physics on the calculated chamber response result was studied and quantitative expressions for their magnitudes were given. Contrary to what had been expected, it turned out that the multiple scattering theory only weakly affected the observed ion chamber response calculation artifacts. Also remarkable was the observation that, for a graphite cavity at ^{60}Co and for ESTEPE = 1%, the error in the implementation of the fictitious method was exactly compensated by the effect of the shortcomings in the PRESTA electron step algorithm, and the magnitude

of the discrepancy between the Monte Carlo calculated response and the expected response was fortuitously equal to the fluence surplus provoked by the PRESTA boundary crossing algorithm alone. The latter observation about that particular algorithm was highlighted earlier in a paper by Foote and Smyth (1995).

In the present paper we study the accuracy of Monte Carlo response calculations of realistic ion chambers free-in-air, in low-energy photon beams (10 to 1250 keV). Four considerations are expected to have significant impact on calculated ion chamber response in this energy region: (i) the consistency of the Monte Carlo code; (ii) the accuracy of the cross-section data used; (iii) the accuracy of the chamber material specification; and (iv) the accuracy of the radiation source. Each of these elements will be discussed in this chapter. Based on the consistency of the EGSnrc results reported herein, the calculation of correction factors to the Spencer-Attix cavity theory was reported by Borg et al. (2000) with the goal of using cavity ionization chambers to measure the air kerma strength of high dose rate (HDR) ^{192}Ir sources.

Fano Theorem And Its Implementation

To check the consistency of the Monte Carlo cavity dose calculations, use was made of the Fano theorem. According to this theorem, under conditions of equilibrium in an infinite medium, the particle fluence will not be altered by density variations from point to point (Fano 1954). For the Fano calculations, an ionization chamber with wall thickness sufficient to provide full build-up was used. For an ionization chamber irradiated with a parallel photon beam in air, according to cavity theory, the dose to the gas in the cavity is related to air-kerma free-in-air by:

$$D_{gas} = K_{air}(1-\overline{g})\left(\frac{\overline{\mu}_{en}}{\rho}\right)_{air}^{wall}\left(\frac{\overline{L}}{\rho}\right)_{wall}^{gas} A_{wall}A_{fl} = K_{coll.wall}\left(\frac{\overline{L}}{\rho}\right)_{wall}^{gas} A_{wall}A_{fl} \qquad (3)$$

where $\left(\frac{\mu_{en}}{\rho}\right)_{air}^{wall}$ is the ratio of mass-energy absorption coefficients of the chamber wall material to air, $\left(\frac{\overline{L}}{\rho}\right)_{wall}^{gas}$, the restricted mass collision stopping power ratio cavity gas (usually air) to wall, $\overline{g}$ the average energy expended in air via radiative interactions, A_{wall} the correction factor for wall attenuation and scattering and A_{fl} the fluence perturbation correction factor. To realize Fano conditions, wall and cavity gas are set to the same material but with a thousand-fold difference in physical density. The density effect correction in the stopping power calculation of wall and cavity material was set to zero by zeroing the International Commission on Radiation Units and Measurements (ICRU) Report No. 37 (ICRU 1984) density effect file involved in the cross section preparation package PEGS4. Hence the restricted mass stopping power ratio in equation (3) is unity. Under Fano conditions, the fluence correction factor A_{fl} is also unity. Hence, from equation (3) under Fano conditions, in order to evaluate the consistency of a Monte Carlo code, the following identity needs to be verified:

$$\frac{D_{cav}}{A_{wall}K_{coll,wall}} = 1 \qquad (4)$$

where cavity and wall consist of the same material [hence a notation different from D_{gas} in equation (3)]. Calculation of collision kerma in the (wall) medium represents a straightforward photon Monte Carlo calculation whereas dose to the cavity represents a full photon-electron transport calculation. We have adopted two methods in evaluating A_{wall}. Firstly, the scheme developed by Rogers and Bielajew (Rogers, Bielajew, and Nahum 1985; Bielajew 1986) was used to explicitly calculate the wall correction factor. Using this technique (in this paper labeled as the conventional technique), A_{wall} is calculated by scoring the primary unweighted dose and the scattered dose in the cavity in a correlated fashion. In principle, using this technique, A_{wall} will be dependent on the accuracy to which electron transport is simulated. However, because of correlations it has always been argued that, although the cavity dose calculation using the EGS4/PRESTA 1.2 system could be wrong, A_{wall} would be largely independent of these calculation artifacts. In this work we also used an alternative technique to verify this possible concern. An equilibrium fluence in the absence of photon attenuation and scattering was calculated by the so-called "regeneration technique": upon a photon interaction, the secondary electron was transported but the (possibly) created scattered photon was removed from the calculation stack and the primary photon was regenerated at the interaction site and allowed to produce new secondary electrons. This technique effectively sets A_{wall} to unity and the cavity dose can be written as $D_{cav,unw}$. In all cases the regeneration technique and the conventional technique were found to give the same unweighted cavity dose, i.e., $D_{cav,unw} = \frac{D_{cav}}{A_{wall}}$.

Materials and Methods

Calculations Under Fano Conditions

Both the EGS4/PRESTA 1.2 and the improved EGSnrc Monte Carlo were tested in comparison with the correct Fano-based result using equation (4). Calculations to test the consistency of these codes were performed for graphite, aluminum, copper, and gold. Calculations were performed using a 1 cm diameter pancake chamber with cavity depth of 2 mm and wall thickness chosen at each energy to be sufficient to provide full build-up. We made use of the user codes CAVRZ and CAVRZnrc for the EGS4/PRESTA 1.2 and the EGSnrc Monte Carlo codes respectively, which both have the option of performing a calculation of A_{wall} with the conventional technique (Rogers et al. 2001). To allow simple calculation of kerma, the photon physics used for these types of calculations was kept to the strict minimum, i.e., we used Klein-Nishina incoherent scattering, no fluorescent photons, and no Rayleigh scattering. Because a large part of the electron transport takes place in the wall, range rejection was used. As well, primary photons were forced to interact at least once in the chamber.

To perform the tests of a Monte Carlo system in a completely consistent manner, all Fano calculations were performed by making use of one single arbitrary set of cross-section data. This means that collision kerma in the wall in equation (4) cannot be simply evaluated using existing data tables for mass-energy absorption coefficients but instead has to be calculated using the same data sets as used in the Monte Carlo system. Collision kerma in the chamber wall and $\overline{g}$ were calculated using separate programs starting from the PEGS4-files used for the chamber response simulations. Based on the simplified photon physics used in the chamber response calculations, total kerma to the wall material or, equivalently $\overline{\mu}_{tr}$ was calculated directly using:

$$\mu_{tr}(E) = \sigma_{pe}(E) + \sigma_{incoh}(E)\frac{\overline{E}_e}{E} + \sigma_{pair}(\mathrm{E})(1 \; - \; 2\; \mathrm{m_o c^2} \; / \; \mathrm{E}) \qquad (5)$$

where $\overline{E}_e$ represents the average Compton electron energy, and the total cross sections of the photon interactions accounted for are denoted by the respective σ. To arrive at collision kerma, the energy lost by bremsstrahlung photons created upon electron slowing down must be calculated for the materials and energies used for the chamber response calculations. We directly calculated $\overline{g}$ by scoring the energy transferred to bremstrahlung photons upon electron slowing down and the total energy transferred by all photon interactions, and calculating the ratio. This was done in a standalone Monte Carlo code, which calls the EGS4 interaction routines, makes use of the EGS4 data sets with the ICRU radiative cross sections, and just scores the desired quantities without physical coordinate transport. Figure 1 shows $\overline{g}$ as a function of energy for carbon, aluminum, and copper for monoenergetic photons between 10 and 1250 keV. As expected, the radiative loss becomes quite significant even at low energies for the higher Z materials.

Measurements and Calculations of Response of Realistic Ionization Chambers

The Exradin A12 (SN 101, SN 149) (Standard Imaging, Middleton, WI) and the NRC 3C (National Research Council of Canada) standard cavity chamber were calibrated against the NRC free air ionization chamber. The NRC 3C chamber is a thick-walled, cylindrical graphite cavity chamber (figure 2) with accurately determined volume and is the basis for the Canadian air kerma standard. The commercial Exradin A12 chamber has C552 plastic wall and central electrode (figure 2). Measurements of the response of the NRC 3C and the Exradin A12 chambers were performed for the X radiation qualities listed in table 1. To this end, the chamber center was aligned with the beam axis and positioned at 1 m from the focal spot (circular field size: 100 cm^2 at the position of the chamber). In addition, measurements were performed at ^{137}Cs and ^{60}Co. At these qualities, the Exradin A12 chamber was provided with a build-up cap, which was not involved in the measurements and calculations at lower energies.

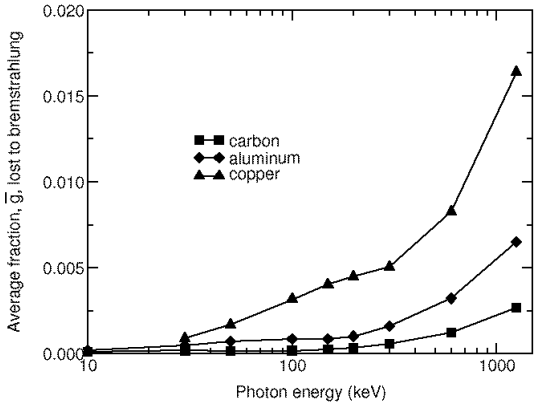

Figure 1. Monte Carlo calculated average fraction of energy lost to bremsstrahlung, $\overline{g}$, for carbon, aluminum, and copper for monoenergetic photons with energies between 10 and 1250 keV.

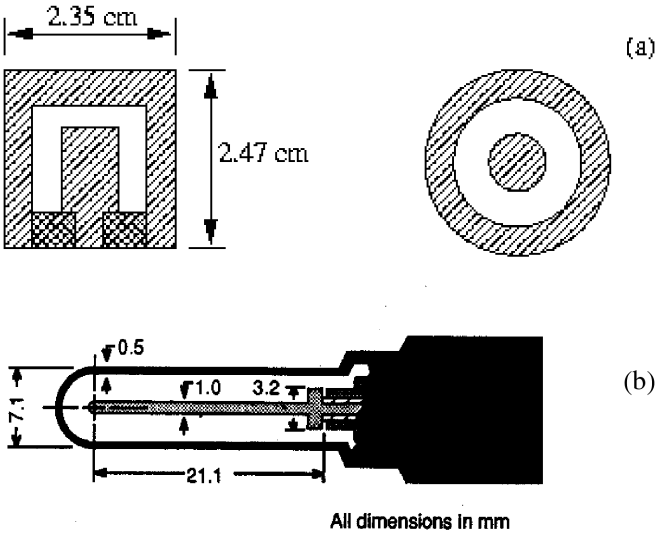

Figure 2. Schematic diagrams of the NRC 3C and the Exradin A12 chambers. The chamber stem was not explicitly modeled in the NRC 3C case. For the Exradin A12, a 2 cm portion of the stem was modeled as a full C552 rod.

For the calculations, the ^{60}Co spectrum was taken from Rogers et al. (1988) and the ^{137}Cs from Walters and Rogers (1998). For the X radiation qualities the spectra were calculated using the program XRAYTUBE (Ma and Seuntjens 1999), which is based on the work of Birch and Marshall (1979). This program calculates the x-ray spectrum emanating from either a W or a Mo target using a parametrization, and estimates the effect of the tube window and filters on the spectrum by simple attenuation. We also used spectra (Seuntjens, Thierens, and Segaert 1987), measured in narrow beam geometry, to investigate the influence of filtration on the calculated response at

Table 1. Characteristics of the kilovoltage beams used to measure the response of the studied chambers. X rays are generated using a Comet MXR-320 X-ray tube (inherent filtration: 3 mm Be). The effective photon energy is derived as the energy of a monoenergetic photon beam having the same half value layer (HVL). The spectra corresponding to these qualities were calculated using the Birch and Marshall (1979) method using the XRAYTUBE (Ma and Seuntjens 1999) program. The response data have been plotted as a function of the mean energies <E>, which are derived from the calculated spectra. The air-kerma rate at the measuring point varied between 0.1 Gy/min at 50 kV and 0.5 Gy/min at 250 kV for the weakly filtered spectra.

kV_p (kV)	Filtration (mm)	HVL (mm)		E_{eff} (keV)	<E> (keV)
		Al	Cu		
50	1.037 Al	1.12	—	22.9	28.3
70	3.11 Al	2.76	—	32.0	39.5
100	4.14 Al	4.40	—	38.5	50.9
150	0.25 Cu,1 Al	—	0.55	62.7	68.2
200	1.029 Cu,1 Al	—	1.10	83.1	86.3
200	1 Pb, 3 Sn, 1 Cu, 1 Al	—	3.99	—	164
250	1.029 Cu,1 Al	—	2.03	109.5	110.9
250	3 Pb, 2 Sn,1 Al	—	5.19	—	208

low energies. For the NRC 3C chamber the stem was not modeled explicitly; for the Exradin A12, a full rod of 2 cm at the basis of the chamber was used to model the stem.

We calculated the response of the NRC 3C chamber and the Exradin Models A12 using the CAVRZnrc user code in the EGSnrc code system (Rogers et al. 2001). Recent improvements in total cross sections, i.e., spin effects, bound Compton scattering and atomic relaxations, discussed by Kawrakow (2000c), were switched on for this part of the work. To ensure the use of the same cross sections for the air kerma part of the calculations, EGSnrc was also used to calculate kerma free-in-air. In this part of the work, this was done by scoring the energy transferred to air at the position of the cavity by primary photons impinging to a thin slab of air. Both calculated and measured response at any radiation quality were normalized to the response at ^{60}Co, i.e., the response at ^{60}Co was used to estimate the effective volume of the chamber.

Results And Discussion

Study of Ion Chamber Response in Low-Energy Photon Beams Under Fano Conditions

Figure 3 shows the response of a carbon Fano cavity at 200 keV as a function of fractional energy loss per step, ESTEPE, as a step length restriction. Since, for this energy, we expected a significant dependence of the EGS4 (standard or PRESTA 1.2) results on the electron transport cutoff (ECUT) (Rogers 1993), calculations were mainly for ECUT and delta electron production threshold, AE 512 keV. It turns out that for carbon at 200 keV, in all cases, the results converge to the correct result at an ESTEPE of 1%. Calculations with the same ESTEPE parameter setting of 1% at other energies show that the values for the EGS4 calculations do not converge to the correct answer and thus the convergence to the correct answer at 200 keV appears to be fortuitous. EGSnrc shows an ESTEPE independent result which agrees with the

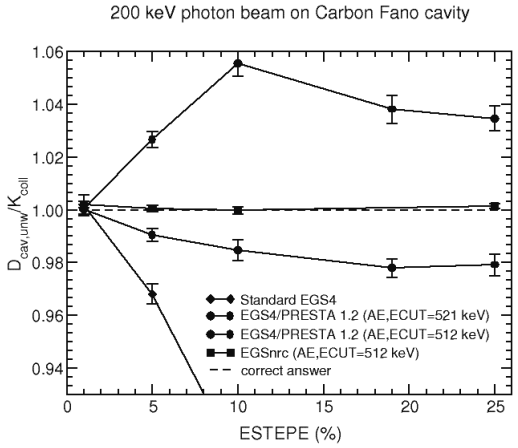

Figure 3. Unweighted response ($D_{cav,unw}/K_{coll}$) of a carbon Fano cavity to 200 keV photons as a function of ESTEPE. Standard EGS4 with AE and ECUT 512 keV, EGS4/PRESTA 1.2 with AE and ECUT 521 keV, EGS4/PRESTA 1.2 with AE and ECUT 512 keV, and EGSnrc with AE and ECUT 512 keV are compared to the exact Fano result (unity).

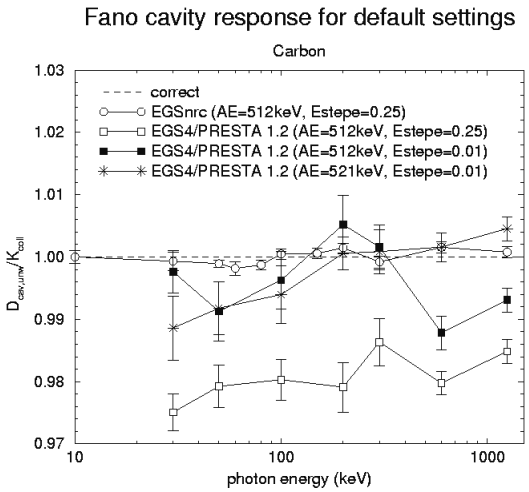

Figure 4. Energy dependence of the cavity calculation artifact for a Fano carbon cavity at a fixed fractional energy loss per step (ESTEPE) unless specified otherwise for ECUT, AE 512 keV. EGSnrc (ESTEPE 25%), EGS4/PRESTA 1.2 (ESTEPE 25%), EGS4/PRESTA 1.2 (ESTEPE 1%), and EGS4/PRESTA 1.2 (ESTEPE 1% with ECUT, AE 521 keV).

expected result within the statistical precision of 0.2% at all transport cutoff thresholds tested.

Figure 4 shows, for a carbon Fano cavity, the energy dependence of the cavity calculation artifact primarily for a transport cutoff of 512 keV and for two extreme values of ESTEPE (1%, 25%). This figure shows that the convergence of the EGS4 results observed in figure 3 is fortuitous: the discrepancies vary between +0.5% and –2.5% depending on energy and ESTEPE restriction whereas EGSnrc appears to produce the correct response at all energies. This result was confirmed for cavities of different materials as indicated in figure 5 where the response of carbon, aluminum, and

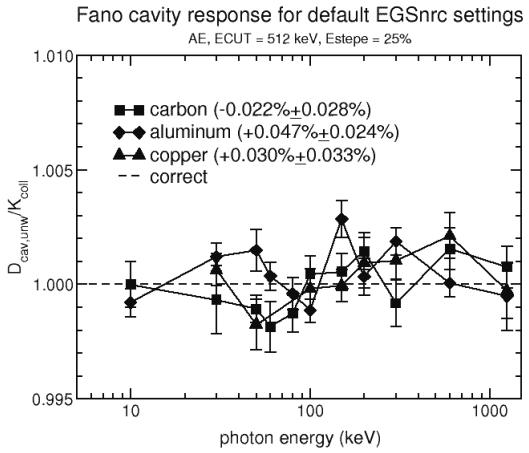

Figure 5. EGSnrc calculated response of carbon, aluminum, and copper Fano cavities as a function of energy for the default fractional energy loss per step of 25%.

copper Fano cavities as a function of energy are shown. We can use figure 5 to make a statement on the consistency of EGSnrc. Averaging the calculated responses at all energies for each of the materials leads to a consistency of –0.02%±0.03% for carbon, +0.05%±0.02% for aluminum and +0.03%±0.03% for copper.

The more elaborate electron step physics together with the fact that boundary crossing is handled in single elastic scattering mode means that for default steplength restrictions (ESTEPE 25%), a cavity dose calculation with EGSnrc is slightly slower than with EGS4/PRESTA 1.2: timing comparisons showed EGSnrc/EGS4(PRESTA 1.2) to be 0.9 to 1.6 depending on the situation tested. However, in order to have any hope for a trustworthy result with EGS4/PRESTA 1.2, a 1% ESTEPE calculation needs to be performed and one really needs to compare EGSnrc(ESTEPE 25%) with EGS4/PRESTA 1.2(ESTEPE 1%). Doing so shows that EGSnrc calculates the correct result with speed improvements of anywhere between a factor of 3 to 13 for the situations tested.

Study of Ion Chamber Response in Low-Energy Photon Beams for Realistic Ionization Chambers

Accurate Monte Carlo calculations of response for realistic ionization chambers, require, in addition to the self consistency of code discussed in the previous section, accurate cross sections, accurate modeling of the geometry and materials, and accuracy in specifying the radiation source. For photon energies lower than 300 keV, a number of observations are important to make in this context. Firstly, for low-Z materials, there is a relatively large proportion of photon scatter (coherent and incoherent) involved in the photon interactions, and the relative effect of atomic binding and relaxations affects the cross sections for these interactions. Secondly, upon going to lower energies, there is an increasing importance of photoeffect (especially in higher Z materials, if present) and hence the accuracy of the photoeffect cross sections is of importance. In addition, the importance of spin effects in the electron multiple scattering modeling was reported to significantly affect the accurate simulation of backscattering and, hence, this should also be taken into consideration when simulating ion chamber response.

In this context, EGSnrc incorporates, in a selectable way, the following improvements in the photon physics: binding effects and Doppler broadening in incoherent photon scattering, improved simulation of photoelectric absorption, and atomic relaxations. In addition, spin effects have been incorporated into the multiple elastic scattering simulation. We tested the relative effect of switching on all the mentioned improvements on calculations of chamber response for the Exradin A12 chamber versus a calculation with all these effects switched off (table 2). The results show an overall effect on the calculated response of the order of at most 1.3%.

Figure 6 shows the measured and calculated response of the graphite 3C cavity chamber as a function of average photon energy of the x-ray spectrum. The first part of the calculations were done for pure graphite as wall material, except for the insulation region between electrode and wall which is polystyrene. The differences between measurement and calculation are less than 0.7% for average energies equal to or larger than 160 keV. Below that energy, the deviations gradually get worse and are up to 9% at average energy of 28 keV (50 kV_p). To put this in perspective, it should be noted that the response change in the studied energy range amounts to 50% as expected for an homogeneous graphite chamber. In an investigation by Barnard et al. (1964)

Table 2. Relative effect of cross section improvements in EGSnrc discussed by Kawrakow (2000c) on the simulation of ion chamber response, $R = D_{gas}/K_{air}$, for an Exradin A12 ionization chamber. R(on): electron multiple scattering distribution with relativistic spin effects, binding effects in incoherent scattering, and atomic relaxations. R(off): screened Rutherford-based electron multiple scattering distribution, Klein-Nishina incoherent scattering, and no atomic relaxations. <E>: average photon energy.

kV_p	<E> (keV)	R (on) / R (off)
50	28.3	1.000 (0.006)
70	39.5	1.010 (0.006)
100	50.9	1.013 (0.005)
150	68.2	1.003 (0.004)
200	86.3	1.002 (0.004)
250	110.9	1.005 (0.004)

at the NPL (National Physical Laboratory, UK) with the goal of using cavity chambers to measure air-kerma in low-energy photon beams, it was found that trace impurities resulting from the machining process of the ion chamber play a dramatic role in the chamber response. For high-Z contaminations on the inside surface of the chamber, the increase in electron fluence due to the rapidly increasing photoeffect cross sections indeed leads to an increased response. We have tried to implement trace impurities in our simulations of the NRC 3C chamber in an effective way. When we implemented a layer of iron on the inside surface of the cavity, we found by calculation that the response of the chamber was a function, in an energy dependent fashion, of (i) the thickness of the layer, and (ii) the area of iron on the inside chamber surface. From a lengthy optimization process it was found that if we implemented an iron ring of thickness 1 μm and inner surface area of 0.45% of the total inner wall area of the chamber into the geometry, the agreement between calculated and measured response is excellent at all energies studied. This case is labeled as "calculation, 1 μm grains of iron" in figure 6, since the same result would be obtained by distributing the iron uniformly in the form of 1 μm diameter grains over the cavity inside

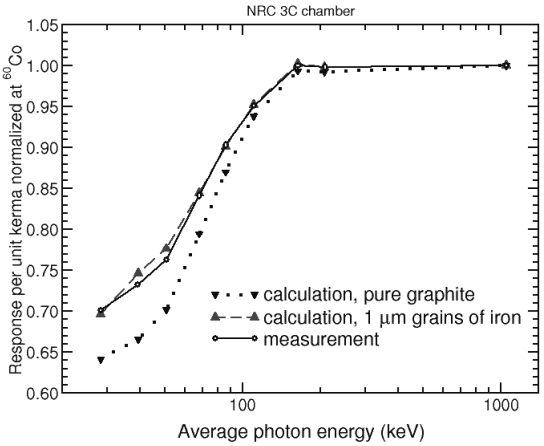

Figure 6. Measured and calculated response of the NRC 3C cavity chamber as a function of average photon energy.

surface. Although this type of comparison does not tell us much about how accurate the calculations are, the amount of contamination found in this iterative process is clearly realistic in view of the machining process of the graphite cavity. A second effect that could increase the response at the lower energies is photon scatter due to the presence of the chamber stem. In this work we have not attempted to model the 3C stem but this would be significant for the lower energy beams (but not the lowest where the photoeffect dominates).

To estimate the effect of impurities on the response of the Exradin A12 chamber, a sample of C552 plastic, the main chamber material, was submitted to mass spectrometry analysis (Laser Ablation Inductively Coupled Plasma–Mass Spectrometry [ICP–MS] by Elemental Research Inc., Vancouver, Canada). Table 3 indicates the ICRU Report No. 37 (1984) composition specification together with the most important elements out of 71 elements analyzed. The amount of impurities with Z values ranging from 10 to 82 was 90 μg/g, or 0.01%. Figure 7 shows the response of the Exradin A12 chamber as calculated with the bare ICRU 37 composition and with the incorporation of the elements as detected by the ICP–MS analysis assumed distributed uniformly throughout the C552 plastic. All calculations are using EGSnrc with full simulation of the improved low-energy photon physics (LEPP). For the ICRU 37 composition C552 plastic, the agreement between measured and calculated response is excellent down to 110 keV mean energy. Below 110 keV calculations and measurements deviate, the calculated response being lower than the measured. Figure 7 shows that the calculated chamber response increases by up to 1% after the implementation of the measured impurities in the composition of C552, extending the excellent agreement down to about 70 keV. The deviations at energies lower than 70 keV may be due to two facts. Firstly, trace impurities on the inside of the chamber wall (not explicitly modeled here) could affect the chamber response, as in the 3C case. This could be the reason for the chamber-to-chamber dependence of the normalized response curves for the two Exradin A12 chambers used. Secondly, at the lower energy X-ray spectra, exact knowledge of the low-energy tail of the spectrum becomes very important. It affects the calculated response critically through the calculation of air kerma, whereas the calculation of cavity dose is less affected since the low-energy photons are easily absorbed in the chamber wall. This is illustrated by the reversed triangles

Table 3. The most significant selection of contaminating elements in C552 as detected by the Laser Ablation ICP–MS technique. The ICRU Report 37 specification of the C552 plastic (in composition by weight) is: H: 2.4%, C: 50.2%, O: 0.5%, F: 46.5%, Si: 0.4%.

Element	Concentration (ppm)
B	17.4
Na	25.0
Mg	9.8
Al	20
P	250
S	12
Ti	3.0
Vn	3.5
Mn	3.4
Fe	70.0
Rb	8.8
Cr	< 50

shown in figure 7 which represent a calculation using two 50 kV spectra with different filtration (0.5 mm Al and 2 mm Al). The change in calculated response by only changing the beam filtration from 0.5 mm Al to 2 mm Al, producing a change in average energy from to 28.6 to 32.0 keV, amounts to 6%.

Finally, an important area of possible improvement in EGSnrc is the use of updated photoeffect cross sections and data interpolation routines that deal properly with these cross sections at characteristic x-ray energies. The default photoeffect data in EGS4 and EGSnrc are based on the Storm and Israel compilation of 1970 (Storm and Israel 1970). Cross sections for photoeffect and pair production in EGSnrc are currently composed, for each necessary material, in the PEGS4 preprocessor and loaded by the code in the HATCH process. Contrary to the total cross sections for incoherent scattering, which are calculated within PEGS4, for the photoeffect and pair cross section, use is made of a datafile (pgs4pepr.dat) where, to a maximum of 61 bins, data are stored for an energy interval ranging from 1 keV to 100 MeV. To implement the more up-to-date cross sections from the National Institute of Standards and Technology (NIST) compilation as provided by the web-based XCOM program (Berger and Hubbell 1987), we implemented the NIST-XCOM data in the pgs4pepr.dat datafile. Figure 8 shows the ratio of the original Storm and Israel data to the NIST-XCOM data for the elements involved in the material air. Except for argon, there is a clear drop in EGSnrc data compared to the XCOM data between 6 and 8 keV. Below those energies the data are not significantly different; above these energies there is a systematic difference that can amount to 10% for some materials. Figure 9 shows ratios of mass-energy transfer coefficients for air calculated, using EGSnrc, with and without the NIST-XCOM data implementation. Energy transfer and hence air kerma with implementation of NIST-XCOM data will be increased compared to the Storm and Israel data. The effect of this cross-section change on Monte Carlo calculated response depends on the materials

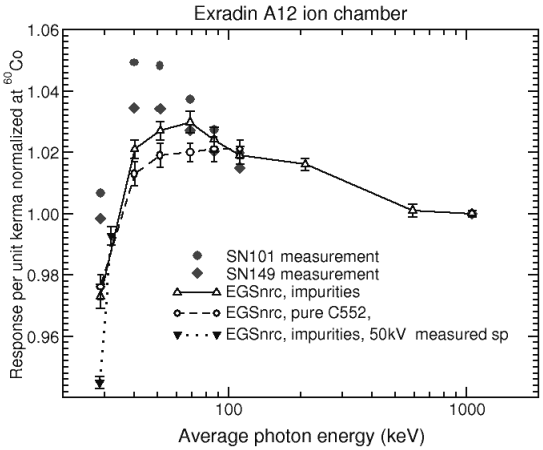

Figure 7. Monte Carlo calculated response of the Exradin A12 chamber type in comparison with measurements for two chambers. Straight triangles: EGSnrc with C552 plastic with spectrometrically determined impurities. Circles: EGSnrc with pure C552 plastic. All calculations are with the EGSnrc cross-section improvements (bound Compton scattering, atomic relaxations, spin effects) switched on (Kawrakow 2000c). Reversed triangles: EGSnrc with C552 plastic with spectrometrically determined impurities using measured spectra with 0.5 mm Al and 2 mm Al added filtration.

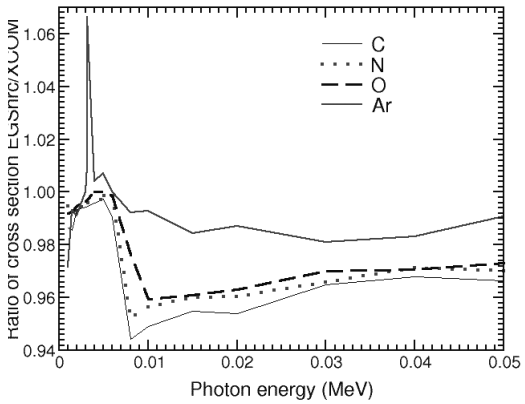

Figure 8. Ratio of photoeffect cross section currently in EGSnrc to the NIST-EXCOM data for typical low-Z elements.

involved in the chamber construction. For a chamber strictly composed of low-Z materials, the chamber response is reduced by about 1%. If, however, there are high-Z elements involved in the chamber construction (as is the case for realistic chambers), the increased probability for photoeffect and the associated increased electron fluence in the cavity could increase the chamber response. A full study of the effect of NIST-XCOM versus Storm and Israel photoeffect cross sections and its effect on important dosimetric quantities as well as ion chamber response exceeds the scope of this chapter and will be published elsewhere.

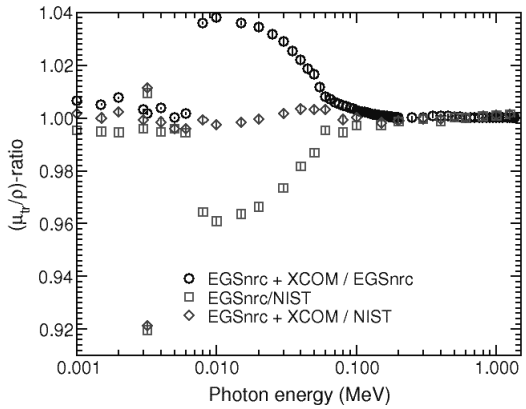

Figure 9. Ratio of mass-energy transfer coefficients for air using the different datasets. Open squares [EGSnrc/NIST]: the ratio of EGSnrc calculated coefficients to those published by Seltzer (1993) and Hubbell and Seltzer (1995). Open circles [EGSnrc + XCOM/EGSnrc]: the ratio of EGSnrc calculated coefficients after the XCOM data implementation to those using the original Storm and Israel (1970) data implementation. Open diamonds [EGSnrc + XCOM/NIST]: the ratio of EGSnrc calculated coefficients after the XCOM data implementation to those using published by Seltzer (1993) and Hubbell and Seltzer (1995).

Conclusions

In this chapter we discussed the accuracy to which ion chamber response in low-energy photon beams can be calculated with the Monte Carlo technique. We first examined the consistency of Monte Carlo calculated ion chamber response in the kilovoltage energy region. To this end we performed ion chamber response calculations for a Fano cavity implementation, where the expected result is known from theory. We compared EGSnrc with its predecessor EGS4/PRESTA 1.2. On average, EGSnrc was found to be consistent to within 0.03% whereas the former EGS version was step-size and transport cutoff dependent from anywhere between –5% to +3%. We then studied ion chamber response calculations in comparison with measurements for two types of chambers, i.e., the NRC 3C graphite cavity ionization chamber and the Exradin A12 ionization chamber. For average energies of 100 keV or higher there is excellent agreement between measured and calculated ionization chamber response. For energies lower than 100 keV, the calculated response is generally lower than the measured response, by an amount that increases with decreasing energy. Of the several possible reasons for this difference, this study investigates three possible explanations. Firstly, the effect on calculated response of trace impurities present in or on the surface of the chamber wall was found to be of the order of 2% for the Exradin A12 chamber and could explain the 8% to 9% difference between measured and calculated response for the NRC 3C graphite chamber. Secondly, the description of the source spectrum needs to be accurate as shown by test calculations with two radiation qualities with very similar average energies. Finally, we tested the overall effect of the improvements in cross sections in EGSnrc (binding effects, atomic relaxations, and spin effects) as well as the effect of changing the photoeffect cross-section datasets to more up-to-date values and found that these improvements affect the response by between 1% and 2%. Other possible areas of improvement not explored in this work could be the inclusion of a more realistic geometry specification (including chamber stem and electric field distribution in the cavity) and the accuracy of photoelectron angular distributions implemented in EGSnrc.

Acknowledgments

At NRC, we acknowledge the support of the National Institutes of Health through grant No. RO1 CA66852. At McGill University, this work was partially sponsored by a grant from the Natural Sciences and Engineering Research Council of Canada (NSERC, RG27800). J.P.S. is a Research Scientist of the National Cancer Institute of Canada supported with funds provided by the Canadian Cancer Society.

References

Barnard, G. P., G. H. Aston, A. R. S. Marsh, and K Redding. (1964). "On the congruity of N.P.L. exposure standards." *Phys. Med. Biol.* 9:333–344.

Berger, M. J., and J. H. Hubbell. "XCOM: Photon Cross-Sections on a Personal Computer." National Bureau of Standards Report, NBSIR 87-3597. Washington, DC: National Bureau of Standards, 1987.

Bielajew, A. F. (1986). "Ionization cavity theory: A formal derivation of perturbation factors for thick-walled ion chambers in photon beams." *Phys. Med. Biol.* 31:161–170.

Bielajew, A. F., and D. W. O. Rogers. "PRESTA: The Parameter Reduced Electron-Step Transport Algorithm for electron Monte Carlo Transport." National Research Council of Canada Report PIRS-0042. Ottawa: National Research Council of Canada, 1986.

Bielajew, A. F., and D. W. O. Rogers. (1987). "PRESTA: The parameter reduced electron-step transport algorithm for electron Monte Carlo transport." *Nucl Instrum. Methods* B18:165–181.

Birch, R., and M. Marshall. (1979). "Computation of bremsstrahlung x-ray spectra and comparison with spectra measured with a Ge(Li) detector." *Phys. Med. Biol.* 24:505–517.

Borg, J., I. Kawrakow, D. W. O. Rogers, and J. P. Seuntjens. (2000). "Monte Carlo study of correction factors for Spencer-Attix cavity theory at photon energies at or above 100 keV." *Med. Phys.* 27:1804–1813.

Fano, U. (1954). "Note on the Bragg-Gray cavity principle for measuring energy dissipation." *Radiat. Res.* 1:237–240.

Foote, B. J., and V. G. Smyth. (1995). "The modelling of electron multiple-scattering in EGS4/PRESTA and its effect on ionization-chamber response." *Nucl. Instrum. Methods* 100B:22–30.

Hubbell, J. H., and S. M. Seltzer. "Tables of X-Ray Mass Attenuation Coefficients and Mass Energy-Absorption Coefficients 1 keV to 20 MeV for Elements Z=1 to 92 and 48 Additional Substances of Dosimetric Interest." NIST Technical Report, NISTIR 5632. Gaithersburg, MD: National Institute of Standards and Technology, 1995.

ICRU (International Commission on Radiation Units and Measurements) Report No. 37. "Stopping Powers for Electrons and Positrons." Bethesda, MD: ICRU, 1984.

Kawrakow, I. (2000a). "Accurate condensed history Monte Carlo simulation of electron transport. I. EGSnrc, the new EGS4 version." *Med. Phys.* 27:485–498.

Kawrakow, I. (2000b). "Accurate condensed history Monte Carlo simulation of electron transport. II. Application to ion chamber response simulations." *Med. Phys.* 27:499–513.

Kawrakow, I. (2000c). "Cross Section Improvements for EGSnrc." World Congress on Medical Physics and Biomedical Engineering, Chicago, July 23–28, 2000.

Kawrakow, I., and A. F. Bielajew. (1998a). "On the representation of electron multiple elastic-scattering distributions for Monte Carlo calculations." *Nucl. Instrum. Methods* 134B:325–336.

Kawrakow, I., and A. F. Bielajew. (1998b). "On the condensed history technique for electron transport." *Nucl. Instrum. Methods* 142B:253–280.

Kawrakow, I., and D. W. O. Rogers. "The EGSnrc Code System: Monte Carlo Simulation of Electron and Photon Transport." National Research Council of Canada Report PIRS-701. Ottawa: National Research Council of Canada, 2000.

http://www.irs.inms.nrc.ca/inms/irs/EGSnrc/EGSnrc.html

Ma, C.-M., and J. P. Seuntjens. (1999). "Mass-energy absorption coefficient and backscatter factor ratios for kilovoltage x-ray beams." *Phys. Med. Biol.* 44:131–143.

Nahum, A. E. "Simulation of Dosimeter Response and Interface Effects" in *Monte Carlo Transport of Electrons and Photons*. T. M. Jenkins, W. R. Nelson, A. Rindi, A. E. Nahum, and D. W. O. Rogers (eds.). New York: Plenum Press, pp. 523–547, 1989.

Rogers, D. W. O. (1993). "How accurately can EGS4/PRESTA calculate ion chamber response?" *Med. Phys.* 20:319–323.

Rogers, D. W. O., A. F. Bielajew, and A. E. Nahum. (1985). "Ion chamber response and A_{wall} correction factors in a ^{60}Co beam by Monte Carlo simulation." *Phys. Med. Biol.* 30:429–443.

Rogers, D. W. O., G. M. Ewart, A. F. Bielajew, and G. van Dyk. "Calculation of Electron Contamination in a ^{60}Co Therapy Beam" in *Proceedings of the IAEA International Symposium on Dosimetry in Radiotherapy.* Vienna: International Atomic Energy Agency (IAEA), Vol. 1, pp. 303–312, 1988.

Rogers, D. W. O., I. Kawrakow, J. P. Seuntjens, and B. R. B. Walters. "NRC User Codes for EGSnrc." NRC Report PIRS-0702. Ottawa: National Research Council Canada, 72 pages, 2001.

Seltzer, S. M. (1993). "Calculation of photon mass energy-transfer and mass energy-absorption coefficients." *Radiat. Res.* 136:147–170.

Seuntjens, J., H. Thierens, and O. Segaert. (1987). "Response of coaxial Ge(Li) detectors to narrow beams of photons for stripping of x-ray bremsstrahlung spectra." *Nucl. Instrum. Methods* A258:127–131.

Storm, E., and H. I. Israel. (1970). "Photon cross sections from 1 keV to 100 MeV for elements Z=1 to Z=100." *Nucl. Data Tables* A7:565–681.

Walters, B. R. B., and D. W. O. Rogers. "Simulation of a Cesium Irradiator Using the BEAM Monte Carlo Code." NRC Report PIRS-. Ottawa: National Research Council Canada, (in preparation), 1998.